SPHERICAL DIRECTIVITY RESONANCE SYNTHESIS

Andrew W. Schmeder

Center for New Music and Audio Technologies
University of California, Berkeley
1760 Arch Street, 94720, CA, USA
andy@cnmat.berkeley.edu

ABSTRACT

The contribution of this paper is the parametric formulation of a sparse representation for synthesizing a signal that has a time-varying spherical directivity component.

This class of signals can be considered conceptually as joint angular-temporal impulse responses on the sphere. Using additive linearity we show how to synthesize these signals from a sparse discrete summation of elementary components that are a linear combination of rotation and scattering operators on the sphere that have reflective and rotational resonant oscillations.

The paper concludes with a discussion of applications of the method to acoustics and spatial auditory scene rendering technologies.

1 Introduction

1.1 Resonance Synthesis

Resonance model synthesis is a method for convolution synthesis of an audio signal with low computational overhead and very low delay by using a bank of second-order resonant filters having a combined impulse response [1],

$$x(t) = \sum_{k}^{N} g_k e^{-\lambda_k t} \sin(\omega_k t + \phi_k). \quad (1)$$

The resonance model shown above, also called an exponentially damped sinusoidal model [2], has a sparse representation given by the set of N tuples of {gain, decay rate, frequency, phase offset}, indicated above by $\{g_k, \lambda_k, \omega_k, \phi_k\}$. The representation can be extracted from data by analysis of the time-varying spectrum of any sound, and the model is sparse when the source is a harmonic resonator such as a musical instrument. To synthesize sound, the model is driven with an excitation signal, such as an impulse or broad-band noise. This audio synthesis algorithm has been shown to produce convincing approximations of the human vocal tract (driven by a glottal impulse-train) and for certain classes of musical instruments where the sparse exponential-decay model is a reasonable approximation of the true impulse response such as bells and plucked strings.

It should be noted that a dense formulation of the synthesis is possible with low latency using partitioned convolution. For very large models this may be more efficient. However, a useful property of the sparse representation is that it enables simple parametric expressive and semantic hybridization transformations (i.e., cross-synthesis, model interpolations, morphs, etc.). In time-domain resonance synthesis this has been used to construct new instruments by mixing attributes of existing instruments in unusual ways, such as overlay of the envelope of one instrument onto the normalized frequency content of an instrument of a very different type [3].

The simple form, flexibility, and ease of use of this algorithm are the source of inspiration for the formulation of a similar method developed in this paper for synthesizing time-varying directivity functions on the sphere.

2 Theory of spherical harmonics

2.1 Modal analysis of spherical functions

Consider a real-valued function $f(\alpha,\beta) \rightarrow \mathbf{R}$ for $(\alpha,\beta) \in S(2)$ where $S(2)$ is the 2-sphere such that f has a finite norm $L^2(S(2))$. For the case of acoustics f is scalar and real-valued but vector and tensor formulations are possible (see Eqn. 2.12 - 2.15 in [4]). The spherical angle is $\Omega = (\alpha,\beta)$ and $d\Omega = \sin(\beta)d\alpha d\beta$. The use of (α,β) in this paper is for consistency with the system of Euler rotation angles that are defined according to the x-convention [5] where the rotation by (α,β) takes the polar axis vector $(0,0,1)$ to the point $(\cos\alpha\sin\beta, \sin\alpha\sin\beta, \cos\beta)$.

The function $f(\Omega)$ as given can be factored into a (possibly infinite) linear sum of orthornormal basis elements called the spherical harmonics. These can be considered conceptually as the natural modes of radial vibration on an ideal spherical membrane, of which there are four basic classes: the radial, zonal, sectorial and tesseral modes. (Figure 1)

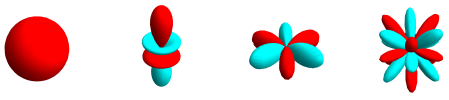

Figure 1: Left to right: radial, zonal, sectorial, and tesseral harmonic modes

When $f(\Omega)$ can be factored into these modes using only a finite number of the basis elements, then f has band-limited directivity. For the sake of simplicity in the remainder of this paper the function $f(\Omega)$ will be assumed to be band-limited.

2.2 The Spherical Harmonics Transform

The transformation of f to the modal domain is possible using the spherical harmonics transform $\mathcal{SHT}$. For f with band-

limited directivity to degree ℓ the forward transform is,

$$\mathcal{SHT}(f) = \{\hat{f}(n,m) : n = 0 \ldots \ell, m = -n \ldots n\} \quad (2)$$

and each coefficient $\hat{f}$ is the inner product with a modal basis element for $S(2)$,

$$\hat{f}(n,m) = \int_{\Omega \in S(2)} f(\Omega) Y_n^{m*}(\Omega) d\Omega \quad (3)$$

where $Y_n^m(\Omega)$ is the complex spherical harmonic of degree n and order m, and $*$ is complex conjugation. The Y functions up to degree 2 are shown in Figure 2.

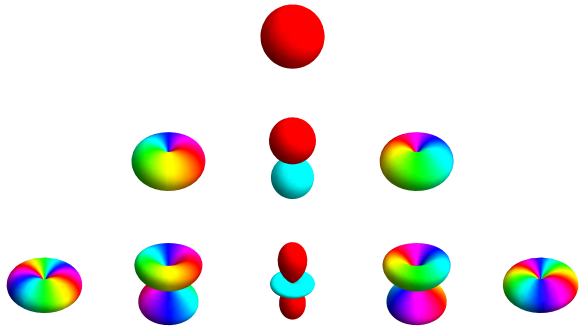

Figure 2: $Y_n^m(\Omega)$ for $n = 0 \ldots 2$ in rows, $m = -n \ldots n$ in columns. The magnitude of Y is shown as radial displacement of the surface, and the color is the phase angle mapped to hue (red = 0, green = $\frac{\pi}{2}$, cyan = π, purple = $\frac{3\pi}{2}$ radians).

The inverse transform $\mathcal{SHT}^{-1}$ can be used to reconstruct f from $\hat{f}$ and it is the discrete summation:

$$f(\Omega) = \sum_{n=0}^{\ell} \sum_{m=-n}^{n} \hat{f}(n,m) Y_n^m(\Omega) \quad (4)$$

This reconstruction is also called synthesis, especially when the coefficients $\hat{f}$ are derived from some parametric process in the modal domain.

The spherical harmonics are the preferred basis for $S(2)$ due to the fact that the application of any linear operator to $\hat{f}$ is still band-limited to the same degree.

2.3 Derivation of the spherical harmonics

2.3.1 Motivation

The most common derivation of the spherical harmonics uses a product of the Legendre polynomials $P(\cos\beta)$ with the Fourier transform on $S(1)$ around α. Here an alternative derivation is shown using a recursive convolution of the Cayley-Klein parameterization for the special unitary group $SU(2)$ with itself. The result is the family of Wigner-D matrices that are the rotation operator on $\hat{f}$ and the center column of which is Y. The advantage of this derivation is that all linear operations on $\hat{f}$ can be formulated as matrix operations, resulting in a more compact mathematical notation.

2.3.2 Cayley-Klein Parameterizationof SU(2)

Let p and q be:

$$\begin{aligned} p &= e^{i\frac{\alpha+\gamma}{2}} \cos(\tfrac{\beta}{2}) \\ q &= e^{i\frac{\alpha-\gamma}{2}} \sin(\tfrac{\beta}{2}) \end{aligned} \quad (5)$$

and the 2x2 unitary matrix U:

$$U = \begin{pmatrix} q & p \\ -p^* & q^* \end{pmatrix} \quad (6)$$

The matrix U is the Cayley-Klein half-rotation parameterization for the special unitary group $SU(2)$ with Euler angles (α, β, γ) [6].

2.3.3 The Wigner-D Matricies

The family of Wigner-D matricies are the rotation operator on $\hat{f}(n,m)$ by the Euler angles $(\alpha, \beta, \gamma) \in ([0, 2\pi] \times [0, \pi] \times [0, 2\pi])$. They are defined for every half-integer degree starting with $U = D_{\frac{1}{2}}$. Any higher order D matrix is given by the recursive definition,

$$D_n = U \bowtie D_{(n-\frac{1}{2})} \quad (7)$$

where $\bowtie$ is the discrete 2D convolution with maximal overhang on both sides (i.e., image convolution with zero padding, see [7]). A normalization is also applied to retain numerical stability (Eqn. 3.2 in [4]).

As an example, the D_1 rotation matrix for degree 1 is:

$$D_1 = \begin{pmatrix} q^2 & \sqrt{2}pq & p^2 \\ -\sqrt{2}p^*q & qq^* - pp^* & \sqrt{2}pq^* \\ p^2* & -\sqrt{2}p^*q^* & q^2* \end{pmatrix} \quad (8)$$

The complex-valued Y_n^m spherical harmonics are found in the central column of the corresponding D_n for n a whole integer and $\gamma = 0$ (Eqn. 2.8 in [4]).

The D_n family for integer-valued n can be applied as a single operator on $\hat{f}$ by formulating a block-diagonal matrix,

$$D = \begin{pmatrix} D_0 & & & \\ & D_1 & & \\ & & D_2 & \\ & & & \ldots \end{pmatrix} \quad (9)$$

The D matrix in this form up to degree 2 with (α, β) free and $\gamma = 0$ is shown in Figure 3 and it is apparent that the central column of each is identical to the rows of Figure 2.

2.3.4 Matrix form of $\mathcal{SHT}^{-1}$

From the block-diagonal form of D, the $\mathcal{SHT}^{-1}$ operation can be given as a dot product with $\hat{f}$ by truncating the sub-matrices of D to their central columns. Let

$$D_Y = \begin{pmatrix} 1 & 0 & 1 & 0 & 0 & 0 & 1 & 0 & 0 & \ldots \end{pmatrix}^T \quad (10)$$

so that,

$$\mathcal{SHT}^{-1}(\hat{f}) = (DD_Y)\hat{f} \quad (11)$$

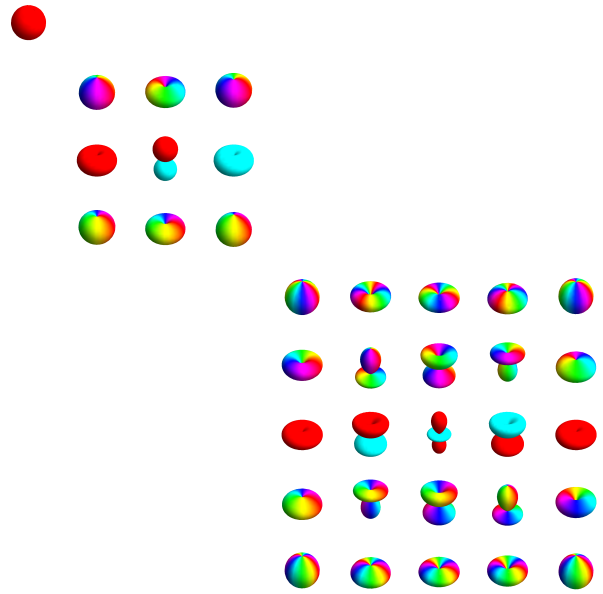

Figure 3: $D(\Omega,0)$ up to degree 2 in block-diagonal form

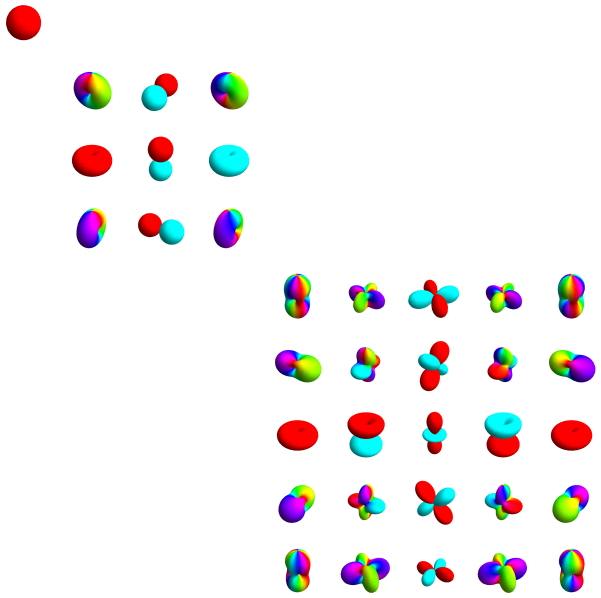

Figure 4: Transformation of $D(\Omega,0)$ to a real-valued basis by C.

2.3.5 Complex and Real Representations

Similar to Euler's formula $e^{i\theta} = \cos\theta + i\sin\theta$ an invertible transformation exists that that takes $\hat{f}$ to a new set of coefficients $\check{f}$ that represents $f(\Omega)$ in a basis of spherical harmonics that are strictly real-valued. This transformation is given by a cross-diagonal matrix C_n with a simple formulation (Eqn. 19 in [8]). Again the C matrix can be formed as a single block-diagonal operator from its components,

$$C = \begin{pmatrix} C_0 & & & \\ & C_1 & & \\ & & C_2 & \\ & & & \dots \end{pmatrix} \tag{12}$$

and,

$$C_{0,1,2} = \begin{pmatrix} \sqrt{2} & 0 & 0 & 0 & 0 & 0 & 0 & 0 & 0 \\ 0 & i & 0 & i & 0 & 0 & 0 & 0 & 0 \\ 0 & 0 & \sqrt{2} & 0 & 0 & 0 & 0 & 0 & 0 \\ 0 & 1 & 0 & -1 & 0 & 0 & 0 & 0 & 0 \\ 0 & 0 & 0 & 0 & i & 0 & 0 & 0 & -i \\ 0 & 0 & 0 & 0 & 0 & i & 0 & i & 0 \\ 0 & 0 & 0 & 0 & 0 & 0 & \sqrt{2} & 0 & 0 \\ 0 & 0 & 0 & 0 & 0 & 1 & 0 & -1 & 0 \\ 0 & 0 & 0 & 0 & 1 & 0 & 0 & 0 & 1 \end{pmatrix} \tag{13}$$

Note that the pattern of sign reversals corresponds to the Condon-Shortly phase convention. The effect of C on D is shown in Figure 4. Using this transform we have the the formula for $\check{f}$:

$$\check{f} = C\hat{f} \tag{14}$$

and,

$$\hat{f} = C^{-1}\check{f} \tag{15}$$

It is therefore apparent that the real and complex forms of spherical harmonics are related by a simple invertible linear operator and are otherwise substantially identical.

2.3.6 Axisymmetric Convolution

Given a function $f(\Omega)$ and a kernel function $k(\Omega)$ such that k is symmetric around its polar axis (i.e., not dependent on α), then a convolution $f \star k$ can be computed in the domain of spherical harmonic coefficients:

$$k \star f = \mathcal{SHT}^{-1}(\hat{k} \odot \hat{f}) \tag{16}$$

And the operator $\odot$ is:

$$\hat{k} \odot \hat{f} = \{\hat{k}(n,0) \times \hat{f}(n,m) : n = 0 \dots \ell, m = -n \dots n\}, \tag{17}$$

and,

$$\mathcal{SHT}^{-1}(\hat{k} \odot \hat{f}) = (\sum_{n=0}^{\ell} \sum_{m=-n}^{n} \hat{k}(n,0)\hat{f}(n,m)) \tag{18}$$

3 Spherical Excitation Signals

3.1 Directivity Impulse

The Dirac-delta function with respect to spherical angle $\delta(\Omega)$ is the impulse function on $S(2)$ (Figure 5). For practical purposes the impulse is band-limited using a low-pass filter w having compact support over degrees $[0,\ell]$ and $w(n) \to 0$ as $n \to \ell$. The δ function can be synthesized directly from the analytic expression of its harmonic coefficients $\hat{\delta}$,

$$\delta(\Omega) = \mathcal{SHT}^{-1}\{\hat{\delta}(n,m) = w(n)Y_n^m(\Omega)\} \tag{19}$$

This also is the basic directivity function used in phase-mode beamforming for spherical arrays of acoustic transducers where the shape of $w(n)$ controls a tradeoff between beam width versus magnitude of beam sidelobes.

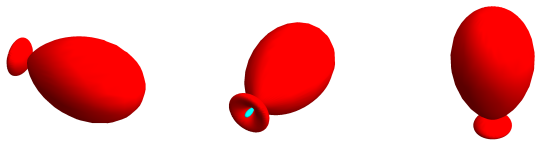

Figure 5: Band-limited Dirac-delta directivity function to degree 3 along x, y and z axes: $\delta(0,\frac{\pi}{2}),\delta(\frac{\pi}{2},0),\delta(0,0)$

3.2 Directivity Noise

A function $x(\Omega)$ with broad-band random directivity can be synthesized by randomizing coefficients for real-valued spherical harmonics. The inverse C operator is used to map these into complex-valued harmonics for synthesis on $S(2)$.

$$x(\Omega) = \mathcal{SHT}^{-1}C^{-1}\{\check{x}(n,m) = w(n)X\} \tag{20}$$

where X is a random variable with uniform distribution on $[-1,1]$ (Figure 6).

Figure 6: Three samples of real-valued random directivity functions band-limited to degree 3

4 Directivity Transformations

4.1 Rotations of Spherical Harmonics

First note that the trivial rotation $D_n(0,0,0)$ is the identity matrix. Rotations of α around the polar axis are given by a diagonal matrix (Eqn. 2.7 in [4]) that is zero except on the diagonal where it is

$$D_n(\alpha,0,0)[m,m] = e^{-mi\alpha} \tag{21}$$

and the notation $D[j,k]$ is the offset row-column index so that $[0,0]$ is the center element of a square matrix with odd-numbered dimensions.

Similarly a rotation by γ is a diagonal matrix,

$$D_{n,m}(0,0,\gamma)[m,m] = e^{mi\gamma}. \tag{22}$$

A rotation by β away from the polar axis not a diagonal matrix. For β in general the matrix is computationally expensive to maintain, however for the case of $\beta = \frac{\pi}{2}$ it is strictly real-valued and has a sparse block-diagonal form. For example, the fixed rotations at degrees 1 and 2 are:

$$D_1(0,\frac{\pi}{2},0) = \begin{pmatrix} \frac{1}{2} & -\frac{1}{\sqrt{2}} & \frac{1}{2} \\ \frac{1}{\sqrt{2}} & 0 & -\frac{1}{\sqrt{2}} \\ \frac{1}{2} & \frac{1}{\sqrt{2}} & \frac{1}{2} \end{pmatrix} \tag{23}$$

$$D_2(0,\frac{\pi}{2},0) = \begin{pmatrix} \frac{1}{4} & -\frac{1}{2} & \frac{\sqrt{\frac{3}{2}}}{2} & -\frac{1}{2} & \frac{1}{4} \\ \frac{1}{2} & -\frac{1}{2} & 0 & \frac{1}{2} & -\frac{1}{2} \\ \frac{\sqrt{\frac{3}{2}}}{2} & 0 & -\frac{1}{2} & 0 & \frac{\sqrt{\frac{3}{2}}}{2} \\ \frac{1}{2} & \frac{1}{2} & 0 & -\frac{1}{2} & -\frac{1}{2} \\ \frac{1}{4} & \frac{1}{2} & \frac{\sqrt{\frac{3}{2}}}{2} & \frac{1}{2} & \frac{1}{4} \end{pmatrix} \tag{24}$$

A general rotation by β can be refactored as a series of elementary rotations:

$$D' = D(0,\tfrac{\pi}{2},0)$$

$$D(0,\beta,0) = \tag{25}$$

$$D(\tfrac{\pi}{2},0,0)D'D(\beta+\pi,0,0)D'D(\tfrac{\pi}{2},0,0).$$

As such it is only necessary to retain $D(0,\frac{\pi}{2},0)$ to compute the rotation of $\hat{f}$ by any element (α,β,γ) in the rotation group $SO(3)$.

4.1.1 Verification of Factorization

Let $A(\alpha,\beta,\gamma)$ be the 3x3 Euler rotation matrix according to the x-convention [5]. A has a trivial decomposition as $A(\alpha,0,0)A(0,\beta,0)A(0,0,\gamma)$. Then,

$$A(\frac{\pi}{2},0,0) = \begin{pmatrix} 0 & 1 & 0 \\ -1 & 0 & 0 \\ 0 & 0 & 1 \end{pmatrix} \tag{26}$$

$$A(0,\frac{\pi}{2},0) = \begin{pmatrix} 1 & 0 & 0 \\ 0 & 0 & 1 \\ 0 & -1 & 0 \end{pmatrix} \tag{27}$$

$$A(\beta+\pi,0,0) = \begin{pmatrix} -\cos\beta & -\sin\beta & 0 \\ \sin\beta & -\cos\beta & 0 \\ 0 & 0 & 1 \end{pmatrix} \tag{28}$$

and,

$$A(\frac{\pi}{2},0,0)A(0,\frac{\pi}{2},0)A(\beta+\pi,0,0)A(0,\frac{\pi}{2},0)A(\frac{\pi}{2},0,0) = \tag{29}$$

$$\begin{pmatrix} 1 & 0 & 0 \\ 0 & \cos\beta & \sin\beta \\ 0 & -\sin\beta & \cos\beta \end{pmatrix} = \tag{30}$$

$$A(0,\beta,0). \tag{31}$$

Therefore, any $A(\alpha,\beta,\gamma)$ can be computed using variable rotations in (α,γ) and a fixed rotation in β by $\frac{\pi}{2}$ radians.

4.2 Scattering Operator

The convolution of f by a kernel k when k is rotationally symmetric around its axis is computed in the modal domain by $\odot$ (Section 2.3.6). Any function f can be reduced to the axisymmetric condition by truncating its modal coefficients to only the zonal harmonics. The zonal harmonics correspond to the coefficients where $m = 0$. Let T denote the zonal truncation

operator as a block-diagonal matrix, e.g.,

$$T_{0,1,2} = \begin{pmatrix} 1 & 0 & 0 & 0 & 0 & 0 & 0 & 0 & 0 \\ 0 & 0 & 0 & 0 & 0 & 0 & 0 & 0 & 0 \\ 0 & 0 & 1 & 0 & 0 & 0 & 0 & 0 & 0 \\ 0 & 0 & 0 & 0 & 0 & 0 & 0 & 0 & 0 \\ 0 & 0 & 0 & 0 & 0 & 0 & 0 & 0 & 0 \\ 0 & 0 & 0 & 0 & 0 & 0 & 0 & 0 & 0 \\ 0 & 0 & 0 & 0 & 0 & 0 & 1 & 0 & 0 \\ 0 & 0 & 0 & 0 & 0 & 0 & 0 & 0 & 0 \\ 0 & 0 & 0 & 0 & 0 & 0 & 0 & 0 & 0 \end{pmatrix} \quad (32)$$

4.2.1 Scattering Kernel from the Dirac Impulse

Let h be the scattering kernel having the form of a circularly expanding wavefront. Intuitively this is the analogue of the Huygens principle as applied in $S(2)$. The scattering kernel is a sub-class of kernels having a simple analytic formula as well as a long-term low-pass convergent behavior (an extension of this work might consider the more general class of complex-valued filters acting on the modal degrees).

This kernel has an analytical formulation by taking the zonal-truncation of a Dirac-delta directivity function after rotation by an angle β. The scattering angle ρ is used for the parameterization of h:

$$\hat{h}(\rho) = TD(0,\rho,0)\hat{\delta}(0,0) \quad (33)$$

or,

$$\hat{h}(\rho) = T\hat{\delta}(0,\rho) \quad (34)$$

For $\rho \in (0, \frac{\pi}{4})$, the action of h is simply a low-pass filter with respect to the modal degree n. The angle controls the steepness of the filter slope. For $\rho \in (\frac{\pi}{4}, \pi)$ the action of h in absolute value is still a low-pass filter, but it has a resonant structure due to complex rotation with periodicity (Figure 7).

4.2.2 Reflection Rate Factorization

A better parameterization of the scattering operator provides control over the rate of reflective oscillation rather than being restricted to periodicity on the integer grid with respect to t. To do this we can transform h into a phase-magnitude form: $h = |h|e^{i\theta t}$.

5 Time Varying Transformations

At this point the theory is sufficient to define a transformation $G(\hat{f},t)$ that produces a time-varying directivity response $g(f,t) = \mathcal{SHT}^{-1}(G(\hat{f},t))$ where the impulse response is recovered when f is the Dirac-delta directivity function $\delta(\Omega)$.

5.0.3 Periodic Rotation

Continuous rotation with rate ω around an axis $\vec{u} = (x,y,z)$, where $\vec{u}$ is at the rotation $D_u = D(\alpha_u, \beta_u, 0)$ away from the pole, is:

$$G_r(\omega,\vec{u},\hat{f},t) = D_u^{-1}D(2\pi(\omega t),0,0)D_u\hat{f} \quad (35)$$

5.0.4 Rate Scattering

Scattering with shape ρ, decay rate λ and reflection rate θ is:

$$G_s(\rho,\lambda,\theta,\hat{f},t) = (|\hat{h}(\rho)|^{\lambda t}e^{i\theta t}) \odot \hat{f} \quad (36)$$

5.0.5 Composition of Transforms

A joint rotational and scattering transform is given by the composition:

$$G_c = G_r(G_s) \quad (37)$$

5.1 Directivity Resonance Synthesis

The total behavior of G is a discrete sum of the previous two types of transformation:

$$G(\hat{f},t) = \sum_k^N G_r(G_s(\hat{f},\phi_k,\lambda_k,\theta_k),\vec{u}_k,\omega_k) \quad (38)$$

A directivity resonance synthesis model is then given by the set of N tuples of (decay rate, scattering shape, reflection rate, rotation vector, rotation rate) notated by $(\lambda_k,\phi_k,\theta_k,\vec{u}_k,\omega_k)$.

The time-domain directivity impulse response is phase-invariant for summations of rotations as in Figure 9 (i.e., is always real for real input), but is complex when scattering exists with resonant reflections.

5.1.1 Recursive Computation

The discrete time-varying synthesis of $g(f,t)$ is possible with a recursive formulation,

$$g(f,t) = g(g(f,t-dt),dt) \quad (39)$$

Therefore the computation is efficient, requiring only the previous state $g(f,t-dt)$ to be stored in memory. At each time slice the output of the model from the previous time is used as the input, and the transformation function g remains static. This demonstrates that the model is a resonant system.

If in addition the source f is a time-varying signal $f(t)$ then the new data integrates additively into the recursive computation:

$$g(f,t) = g(g(f(t-dt),t-dt)+f(t),dt) \quad (40)$$

An example of the computation at multiple time slices is shown in Figures 8 and 9.

6 Applications in Acoustics

6.1 Ambisonic Transformations

Ambisonics is a practice in audio engineering whereby loudspeakers are distributed on a spherical shell for the reconstruction of the interior sound field. It also involves sampling of acoustic spaces with spherical microphone arrays, typically having a compact ball geometry.

The formulation of directivity transformations by the scattering and rotation operators may provide an answer to the question of how to definine the class of valid ambisonic transformations in a more general way [9]. In particular it may be useful to parameterize a reverberation effect for the ambisonics domain that is true to the geometry of the sphere.

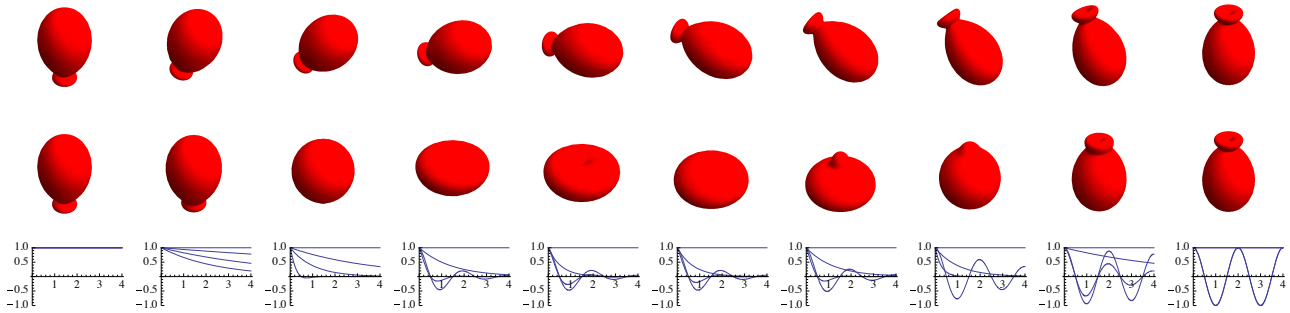

Figure 7: Top row: Rotations of the Dirac-dirac directivity function away from the polar axis, $D(0,\beta,0)\hat{\delta}(0,0)$ for $\beta \in [0,\pi]$. Middle row: Axisymmetric scattering kernel obtained by truncating the above to the zonal harmonics, $\hat{h}(\rho) = TD(0,\rho,0)\hat{\delta}(0,0)$. Bottom row: Real-part of decay in modal coefficients per degree n versus time t.

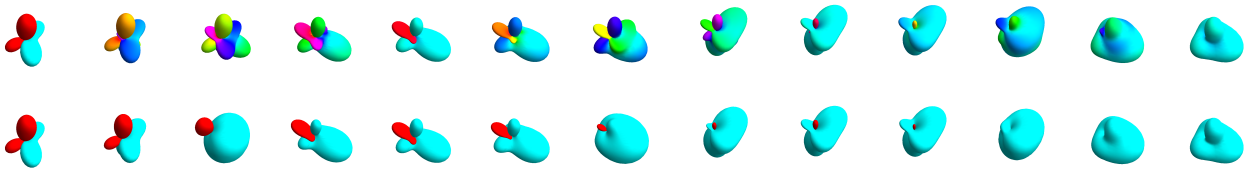

Figure 8: Top row: Complex-valued response of a scattering kernel with resonant reflections $G_s(\frac{4\pi}{6}, \frac{4\pi}{6}, \frac{1}{4})$, excited from random initial conditions. Note a reflection occurs every time the signal has zero imaginary component. Bottom row: Normalized real-part of the above response.

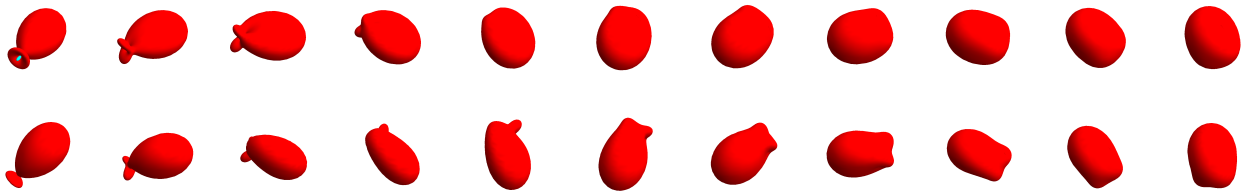

Figure 9: A directivity resonance model consisting of sum of two orthogonal rotations $G_r(\frac{\pi}{4},(1,0,0)) + G_r(\frac{\pi}{4},(0,1,0))$. Top row: impulse response from $\delta(0,\frac{\pi}{2})$. Bottom row: impulse response from $\delta(\frac{\pi}{4},\frac{\pi}{4})$. Observe that the decay rate of higher-degree harmonics is faster when the direction of the exication impulse is coincident with an axis of rotation (as in the top example) and slower otherwise (bottom).

6.2 Room Impulse Response Analysis

Thus far we have considered only the generative synthesis of directivity resonance models. It is natural to consider a possible analysis method for extracting such models from recorded data. This may require the introduction of more a sophisticated model, for example by including time-delay structures as in the damped-delayed sinusoidal model [2]. Unfortunately this approach may have limited utility since rooms are not spherical in shape and so a room impulse response is not band-limited in $\mathcal{SHT}$ (plane waves are not band-limited in directivity), thus the estimation could have a large error.

6.3 Auditory Scene Synthesis

Compact spherical loudspeaker arrays can reproduce high-degree directivity patterns in real-time [10]. In addition the simulation of source directivity is possible in wave field synthesis [11] and headphone auditory display systems.

Currently many systems implementing source directivity are parameterized by static descriptions of beam shape and orientation. This parameterization is adequate for some existing applications such as computer gaming. However the methods shown here provide a means to express dynamic directivity systems that respond to input in real-time. For example a directivity resonance model could be used to synthesize the directivity component of a physical instrument model that is excited directionally using a haptic controller [12].

6.4 Perception of Directivity

An informal study on the usable range of rotation frequencies for a Dirac-delta beam was carried out in [12]. From this information it is reasonable to conclude that all directivity effects need to occur at sub-audible frequencies to avoid perceptual fusion (up to about 10 Hz), and that rotation rates should be controlled on a log-scale to map to a relatively linear perceptual effect.

7 Acknowledgements

Thanks to Meyer Sound Laboratories Inc. of Berkeley CA for financial support.

8 References

[1] X. Rodet, "Time-Domain Formant-Wave-Function Synthesis," *Computer Music Journal*, vol. 8, no. 3, pp. 9–14, 1984. [Online]. Available: http://www.jstor.org/stable/3679809

[2] R. Boyer and K. Abed-Meraim, "Damped and delayed sinusoidal model for transient signals," *IEEE Transactions on Signal Processing*, vol. 53, pp. 1720–1730, May 2005.

[3] Y. Potard, P.-F. Baisnée, and J.-B. Barrière., "Experimenting with Models of Resonance Produced by a New Technique for the Analysis of Impulsive Sounds," in *Proceedings of the ICMC*, La Haye, 1986.

[4] T. Risbo, "Fourier transform summation of Legendre series and d-functions," *Journal of Geodesy*, vol. 70, no. 7, pp. 383–396, 1996.

[5] W. Mathworld, "Euler Angles," http://mathworld.wolfram.com/EulerAngles.html, 2010.

[6] ——, "Cayley-Klein Parameters," http://mathworld.wolfram.com/Cayley-KleinParameters.html, 2010.

[7] Wolfram Research Inc., "List Convolve - Wolfram Mathematica 7 Documentation," http://reference.wolfram.com/mathematica/ref/ListConvolve.html.

[8] M. A. Blanco, M. Flórez, and M. Bermejo, "Evaluation of the rotation matrices in the basis of real spherical harmonics," *Journal of Molecular Structure: THEOCHEM*, vol. 419, no. 1-3, pp. 19 – 27, 1997. [Online]. Available: http://www.sciencedirect.com/science/article/B6TGT-409W1GH-4/2/fe118319442ea79641542aa6ba293846

[9] M. Chapman and P. Cotterell, "Towards a Comprehensive Account of Valid Ambisonic Transformations," in *Ambisonics Symposium*, 2009.

[10] R. Avizienis, A. Freed, P. Kassakian, and D. Wessel, "A Compact 120 Independent Element Spherical Loudspeaker Array with Programmable Radiation Patterns," Paris, France, 2006, p. Convention Paper No. 6783.

[11] E. Corteel, "Synthesis of directional sources using wave field synthesis, possibilities, and limitations," *EURASIP J. Appl. Signal Process.*, vol. 2007, no. 1, pp. 188–188, 2007.

[12] A. Schmeder, "An Exploration of Design Parameters for Human-Interactive Systems with Compact Spherical Loudspeaker Arrays," in *Ambisonics Symposium*, 2009.